JP&M Engineering
Journal of Petroleum and Mining Engineering

A New Vision for Hydrocarbon Trapping of Alam El-Bueib Formation in Aman Oil Field Using Fault Seal Analysis Technique, Northern Western Desert, Egypt

Nabih, M. [a*], Ghoneimi, A. [a], Essa, A. [b] and Saleh, A. H. [a]
[a] Zagazig University, Faculty of Science, Geology Department, 44519, Zagazig, Egypt
[b] Agiba Petroleum Company, Cairo, Egypt
*Corresponding author e-mail: mnabih@science.zu.edu.eg

Article Info

Received: 2 Feb. 2023
Revised: 17 Feb. 2023
Accepted: 26 Feb. 2023

Keywords

Fault seal analysis; 3D seismic structural modeling; Meleiha concession; Alam El-Bueib Formation; Aman oil field.

Abstract

This study aims to overcome the problem of unexpected hydrocarbon non-potentiality detected in Alam El-Bueib (AEB) member in Aman field. To achieve this objective, the structural framework and petrophysical analysis of the studied interval is carried out using seismic and well log data, respectively, then using the fault-seal analysis technique to assess the availability of the main fault dissecting AEB Formation to trap hydrocarbons. Structure depth contour maps and 3D structural model are constructed for illustrating the main structural features to assign and evaluate the most promising locations of closures favorable for hydrocarbon trapping. AEB III-E shows a general dipping to the northwest and south, constituting a horst fault-block dipping to the northwest. These structural settings are mostly three-way dipping and occasionally four-way dipping closures and accomplish the conditions for trapping of hydrocarbons. AEB III-E sandstone shows a porosity of 14 % to 16 % and water saturation near to 100 %, as reported by JASMIN-1X (J-1X) well. Fault seal analysis revealed that the main fault dissecting AEB Formation near J-1X well represents a leakage zone for hydrocarbon movability and its un-trapping in the location around the well. Finally, due to the good quality of AEB Formation in the study area ant its surroundings, a prospects prediction routine is carried out to search for other prospects. Two prospects are predicted which may be more favorable for hydrocarbon trapping.

1. Introduction

Five essential elements must exist in any petroleum system for a hydrocarbon prospect to exist. These main elements are the source rock, reservoir rock, seal rock, the trap and finally timing to permit all those processes of generation, migration, accumulation, and preservation to occur [1-2]. Aman oil field is located in the northern portion of the Western Desert at 60 km south of the Matruh coast, between X: 709200 and 719600 mE and Y: 294000 and 282800 mN (Lat. 30° 03' and 30° 54' N and Long. 27° 00' and 27° 18' E) (Fig. 1). Bahariya Formation is the main producing reservoir in this field. Aman-1X was the first well drilled in the area by Agiba Petroleum Company in May 1985 to test the oil potentialities of the Bahariya sand reservoirs [6].

Aman oil field occupies an area between Matruh and Shushan basins located in the northern Western Desert. These basins were upturned in the Late Cretaceous to Early Tertiary, resulting in the formation of the NNE-SSW directed fault dissemination folds that were then anatomized by the NW-SE normal faults. These folds form excellent hydrocarbon traps throughout the area and surroundings. In addition, normal faults of mainly NE-SW trend and tilted fault blocks of the WNW-ESE main trend, form the main structural traps occupying these basins [7-8]. Numerous oil and gas fields have been found in the Shushan and Matruh basins, where the source rock of the Jurassic age is present. One of these fields is the Aman oil field [6]. The AEB Formation in several oil fields is one of the main reservoirs where, the rocks of AEB Members act as sources, caps, and reservoirs in several basins in the Western Desert. One of the primary oil-bearing members of the Western Desert's AEB Formation is the AEB-III-E Member [9-14].

The 3D modeling technique, based on well log and seismic data to investigate the structural characteristics of reservoirs, had been carried out by many authors such as [15-18]. Utilizing the 3D structural modeling technique achieves the main

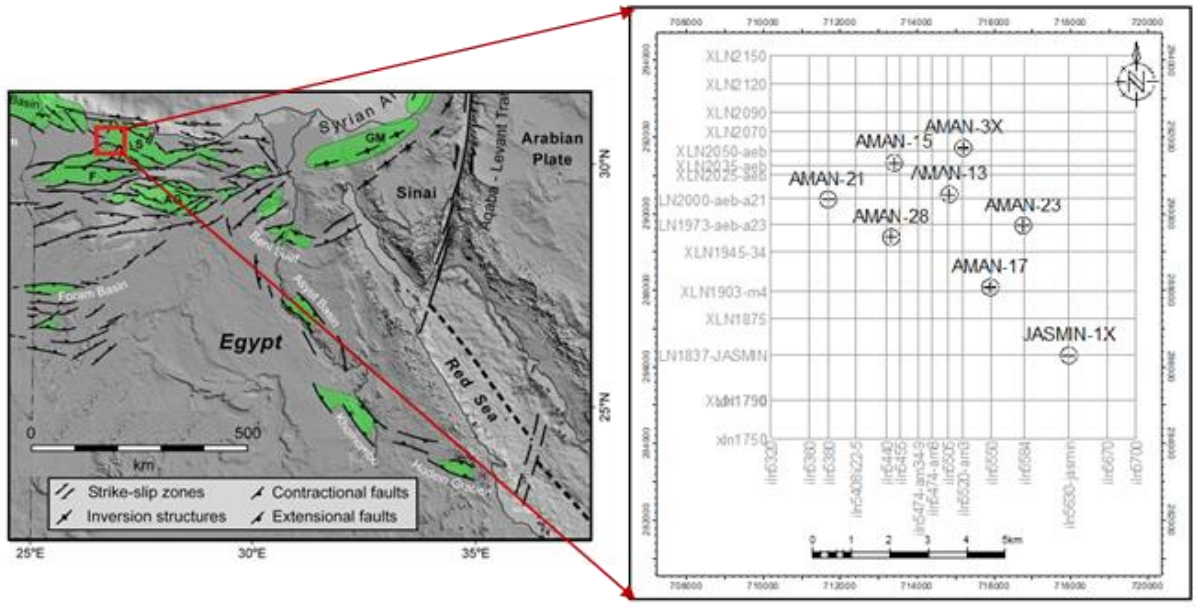

(a) **(b)**

Figure 1. (a) Location map of Jurassic and Cretaceous rift basins in the Western Desert of northern Egypt (Orang box). Onshore background image is the [3] digital terrane model. Offshore image is [4] Seasat-derived bathymetry. Faulting and basin geometry (green) is after [5]. AG = Abu Gharadig basin; F = Faghur basin; GM = Gebel el Maghara; S = Sushan basin, **(b)** Aman oil field map showing locations of the seismic grid and wells.

advantage of the capability for modeling complex structures. This investigation clarifies the importance of fault seal analysis in the re-decision process for the hydrocarbon potentiality of AEB-III-E Member and to locate better positions for hydrocarbon accumulation at the main potential reservoir layers in Aman oil field, as well as to propose other unexplored prospects for the field development.

2. Geological Setting

The sedimentary basins of the northern Western Desert were highly structurally controlled by faults which are mainly determined from regional magnetic, gravity, seismic, and wells data [19]. This leads to the high diversity of rock facies being deposited. The majority of these faults have a long growth history and suffered from strike-slip movements [20]. The African plate lateral movements affected these faults during the Jurassic (sinistral) and late Cretaceous (dextral) [21]. Most folds of the Late Cretaceous-Early Tertiary of the northern Western Desert are compressional and have a NE-SW trend as shown in the Abu Roash area. Other folds, due to horizontally displaced or normal faults, are confined to fault blocks of axes that are oblique, parallel, or perpendicular to the fault block [22; 19].

Figure (2) shows the simplified thick stratigraphic section of the northern Western Desert which consists of a sedimentary sequence ranging from Pre-Cambrian to Recent [9; 23]. The AEB Formation (Early Cretaceous Neocomian-Barremian) is composed predominantly of sandstone intercalated with siltstone and shale and sometimes thin limestone and dolomite beds [19]. Many studies were carried out on the northern Western Desert regarding the stratigraphy, facies distribution, tectonic framework, and hydrocarbon potentialities [2; 8; 10; 24-30].

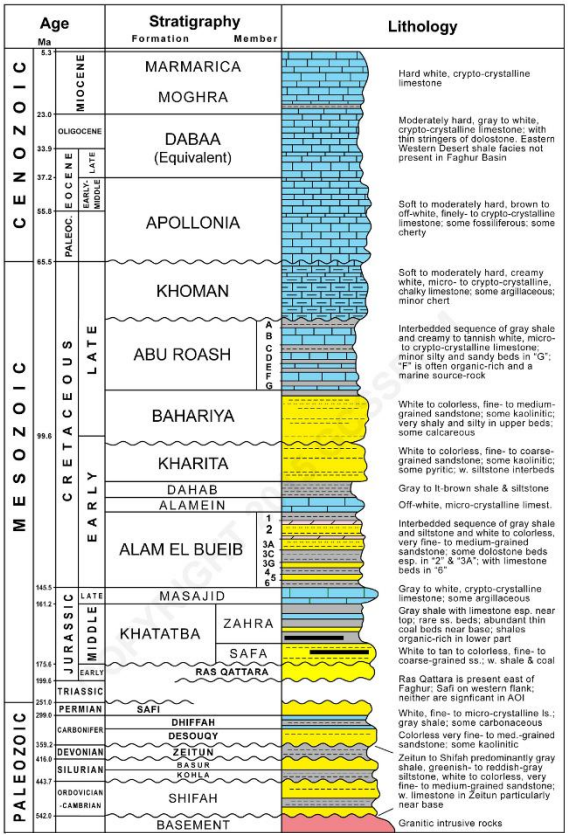

Figure 2. Simplified stratigraphic section of the northern Western Desert [6].

3. Materials and Methodology

The seismic data is represented as a set of thirty seismic sections (2D) derived from a 3D seismic data volume. These sections are divided into fifteen inline directed N-S and fifteen crosslines directed E-W. In addition, the data from 8 wells are used for carrying

out the seismic interpretation. All these wells had bottomed in Bahariya Formation, except the J-1X well which reached to Ras Qattara Formation. The J-1X well is an exploratory (wildcat) well and penetrates the AEB Formation. Well logs data of the J-1X well (caliper, GR, density, PEF, neutron, and resistivity) are available for this work where the AEB Formation is studied to evaluate the petrophysical parameters of the AEB-III-E Member. This work passed through four steps to achieving our aim of clearing how much the sealing or leaking windows is a very important agent in oil and gas reservoir evaluation and development of sprawling counties. The successive work steps are shown in the shape of workflows. These steps are seismic interpretation for 3D modeling of the reservoir, well log analysis for petrophysical evaluation, fault seal analysis, and finally prospects detection and oil-in-place estimation. The seismic interpretation workflow includes several steps including the reflectors identification using the available well data, time-depth relations and stratigraphic information from the available wells, picking of reflectors and fault locations, closing loops, contouring of time values on horizons, velocity mapping, and finally the time to depth conversion to contour structural maps and finally constructing three 3D structural models. The time-depth (T-Z) curve available in the J-1X well is used as the time-to-depth relation in this study. The average and interval velocity values of the different and successive horizons (units), members, and formation in these well estimated and curves plotted.

4. Results and Discussion

4.1. Seismic analysis

Seismic data can be analyzed according to the required investigation. These analyses such as deformed structure can be geometrically analyzed in the hydrocarbon reservoirs [31- 32], Crustal architecture analyses [33-37], Strain Analysis [38], and progressive deformation analysis which is important in trapping and sealing of faults reduction analysis as faults reactivate. The timing of the formation of traps vis the timing of hydrocarbon generation is also matched to understand the charging of the reservoir [39-40]. Examining the seismic sections as a whole can help determine the broad pattern of structural characteristics of interest before beginning any detailed seismic interpretation work [41]. The seismic polarity for used data reflects a normal polarity, where the increasing of acoustic impedance gives a peak and the decreasing gives a trough. The seismic signature is defined and started from the created synthetic seismogram (Fig. 3) and continued across the area according to the expected and possible variation of the geological factors such as lithology. Seismic sections were interpreted in terms of horizons (AR-A, AR-G, Bahariya, Alamein, AEB-III-E, Masajid, and Khatatba) and faults segments were picked. Two composite seismic sections (Figs. 4a and b) are represented to illustrate the seven picked horizons and detected faults. It is noted that fault number F1 is repeated four times crossing the composite seismic since this composite seismic section is nearly zigzag-like and Fault F1 intersects the composites section at four positions. These selected seismic sections pass through the available wells, to facilitate and control the picking process. The first composite seismic sections are mainly oriented E-W (Fig. 4a) and the second composite seismic sections are mainly orientated N-S (Fig. 4b). The picked AEB III-E top is nearly horizontal to gently dipping. Four normal high dipping faults (F1, F2, F5, and F7) are detected and two of them (F1 and F2) are the main faults crossing the picked top.

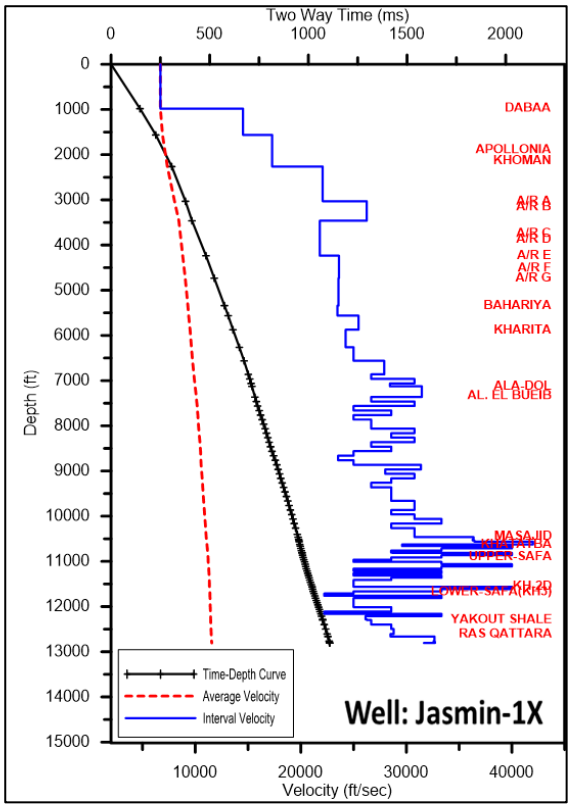

Figure 3. Time-depth relation of J-1X well with the unit top.

The isochronous map of the AEB-III-E top generated using its two-way time (TWT) values which displays that the highest value is 1545 ms is existed in the southeastern part of the area, while the lowest value is 1650 ms is existed in the southeastern and the northern parts (Fig. 5). The time depth relation of the J-1X well is used to convert the isochronous map into a depth structure contour map on the top of the AEB-III-E Member. The depth map at the top of AEB-III-E Member shows that the highest value -7940 ft is located in the southeastern part of the area, and the deepest value -8420 ft is located in the southeastern and northern parts of the area (Fig. 6).

As shown in Figures (5 and 6) the linkage area between the fault segments F1 and F5 is graben where F1 throws to the south while F5 to the north. The same is for the linkage area between F2 and F7 is mostly graben except at the northern part of the linkage area which rises to form a pattern like relay ramps. Four faults dissect the top with a main trend of

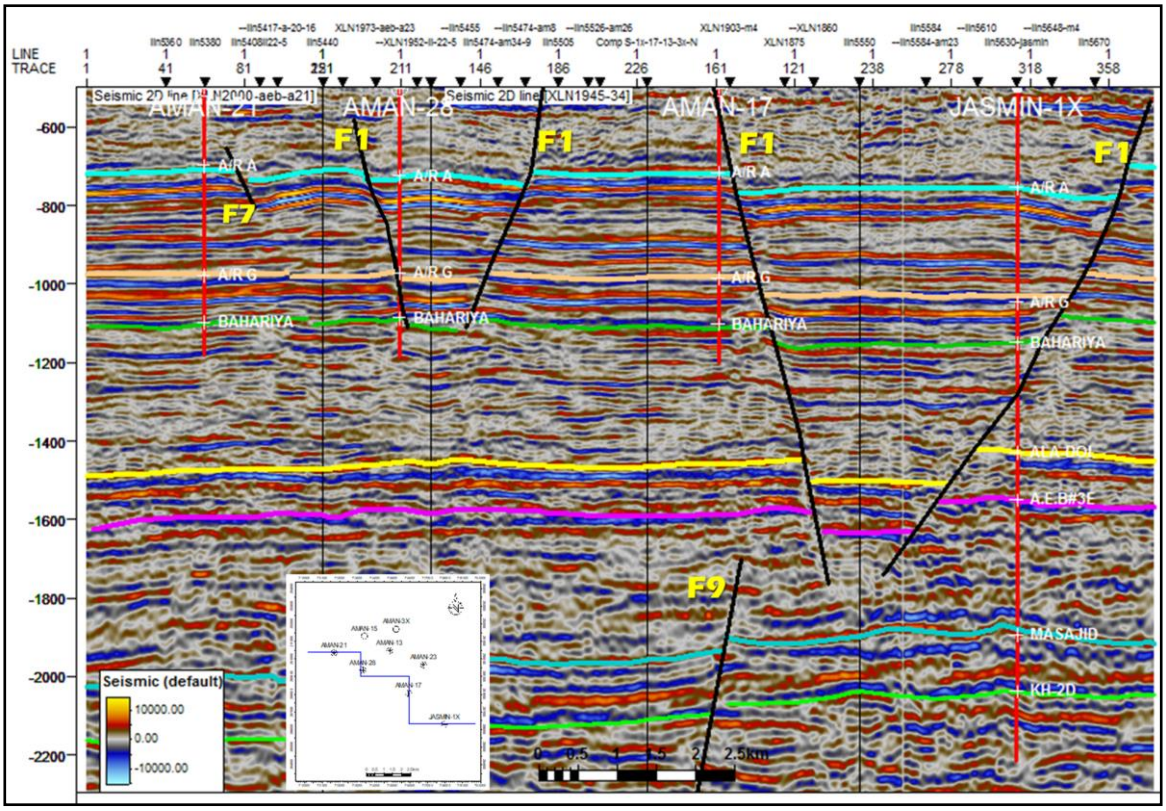

(a)

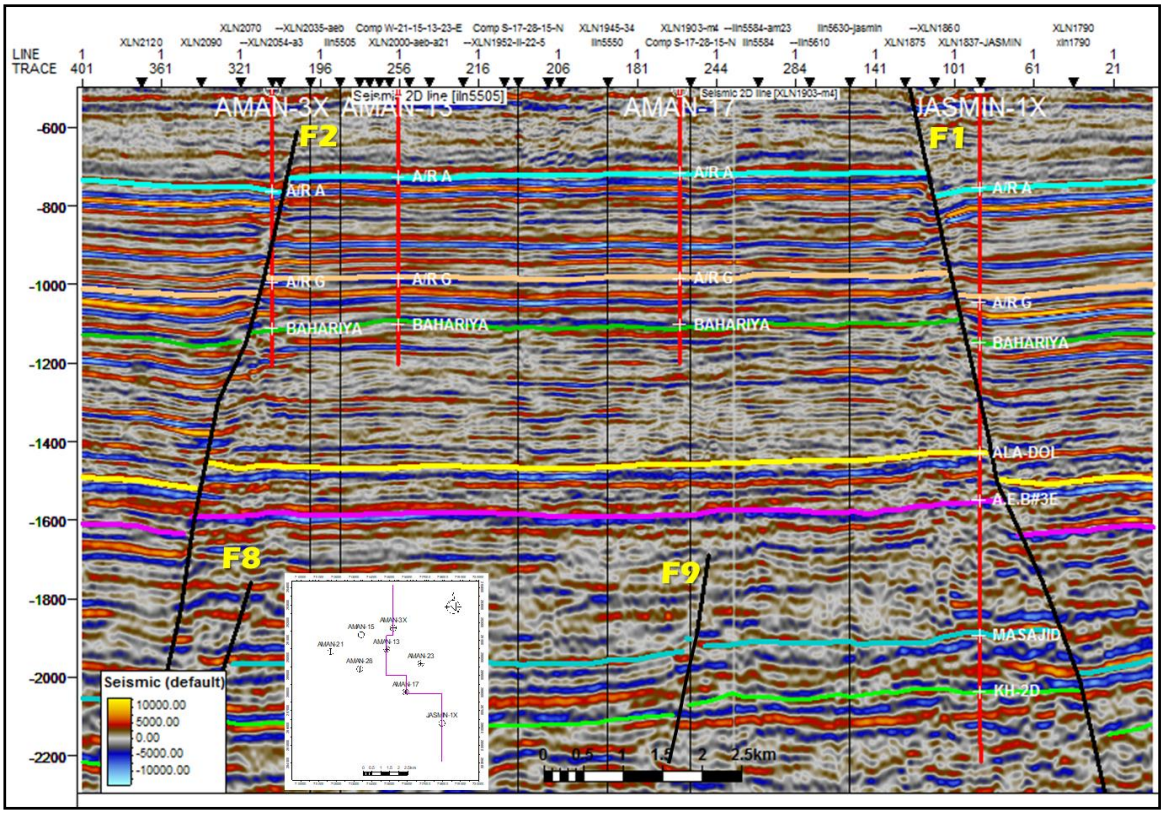

(b)

Figure 4. Interpreted East-West composite seismic section passing through boreholes AMAN-21, 28, 17 and J-1X **(a)** and North-South composite seismic section passing through boreholes AMAN-3X, 13, 17 and J-1X **(b)**.

NW-SE. Fault F1 is throwing to the SW. Faults F2, F5, and F7 are throwing to NE. The combination of these faults forms a horst. For example, faults F1 with F2 form horst in the middle part. These horsts may constitute the most petroleum traps in the area. The major two normal faults (F1-F2) are trending NW-SE bound the structure in the middle and the southern producing horst block shifting the highest point to the southern part. The major two normal faults (F1-F2) are trending NW-SE and bound the structure in the middle and the southern producing horst block shifting the highest point to the southern part.

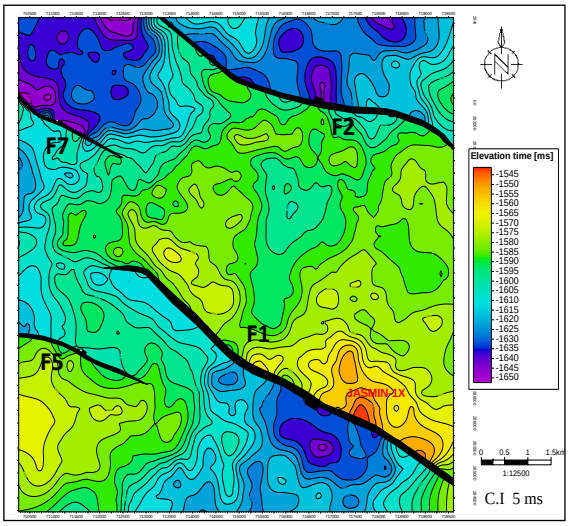

Figure 5. Isochronous map on top of AEB III-E.

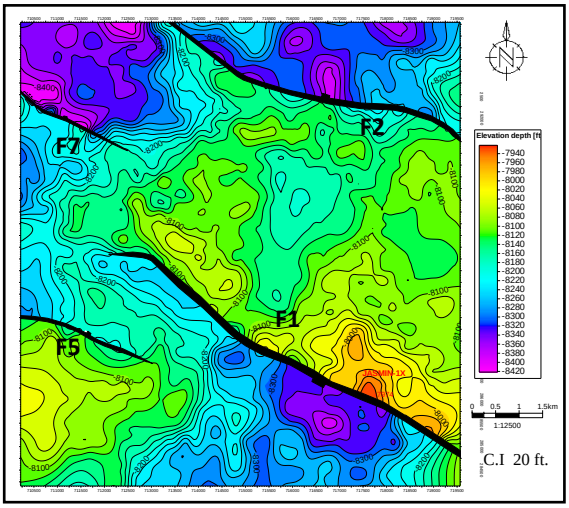

Figure 6. Structure contour map on top of AEB III-E.

The borehole data of the studied wells and the thirty seismic sections derived from a 3D seismic volume are integrated to construct a 3D structural model. The 3D seismic structural modelling technique passes through the three steps in the workflow shown in Figure (7). This model represents a general view of the subsurface lateral and vertical configuration of the studied AEB reservoir (Fig. 8). It represents the configuration of the AEB Formation top between faults F1 and F2 which constitutes the extension of the horst shown upward and downward. The well J-1X is located in the fault F1 upthrown side and penetrates the AEB Formation top at the highest area of the F1-F2 horst block. It also shows that fault F7 is shifted to the north and bounds the lowest part of this top. The model highlights the structural features on the tops of studied formations and shows clearly the magnitude of fault throws.

4.2. Well logs analysis

The normal logs of the caliper, bit size, GR, PEF, density, neutron, and resistivity in the eight wells are used for the formation evaluation of the studied AEB-III-E reservoir. The petrophysical parameters estimated from the well-log analysis are shale content, porosity, lithology, and water saturation. The procedures used for well-log interpretation are based on equations and charts of Schlumberger, [42; 43] and Bateman, [44].

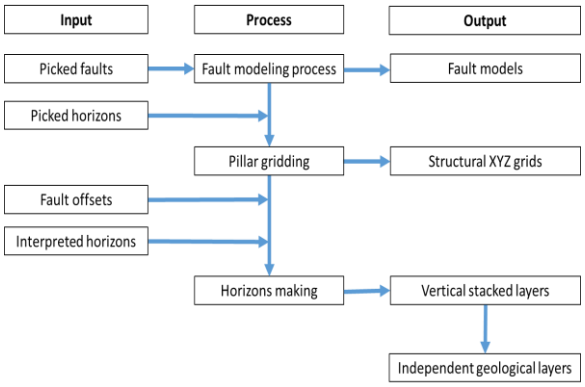

Figure 7. Workflow used for constructing the3-D structural model of AEB Formation.

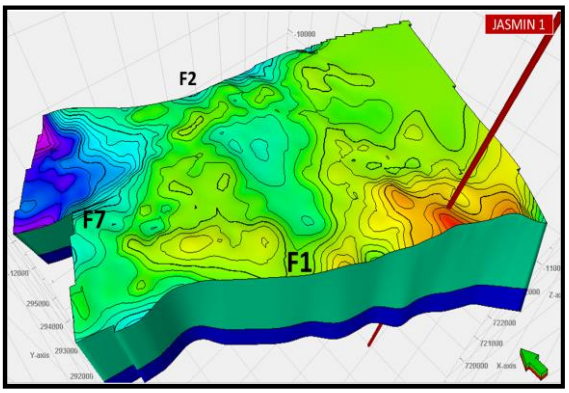

Figure 8. 3-D structural model of AEB Formation.

The well log analysis is summarized as a workflow based mainly on the equations and charts of Archie, [45]; Schlumberger, [46]; Dake, [47]; Dresser Atlas, [48] and Crain, [49] (Fig. 9). The workflow starts with well log data input, editing basic well log analysis and finally, the formation evaluation. The basic well log analysis steps start from the estimation of shale volume from the gamma-ray log, and porosity from the density-neutron logs combination. The porosity is corrected for shaliness to estimate the effective porosity which is used to calculate the water and hydrocarbon saturation. Finally, the initial oil in place is calculated. The well-log analysis reflected that the AEB-III-E Member consists mainly of sandstone with siltstone zones and shale zones which is a suitable environment for hydrocarbon accumulation. The AEB-III-E is underlie the AEB-III-D where its bottom shale acts as cap rock (Fig. 10).

The AEB-III-E Member plays a promising reservoir in several areas of the Western Desert [6; 50]. There is no hydrocarbon potentiality in the AEB-III-E Member in the J-1X well and this is contrary to expectations in the concession under study. The analysis shows that AEB-III-E Member has about 362 ft reservoir thickness with porosity of about 16 % and water saturation near 100 %. The analysis shows that there is no hydrocarbon potentiality (Fig. 10). In addition, this well is not produced from this reservoir which has good petrophysical characteristics as mentioned above, this is another piece of evidence. Therefore, it is necessary to re-study from another

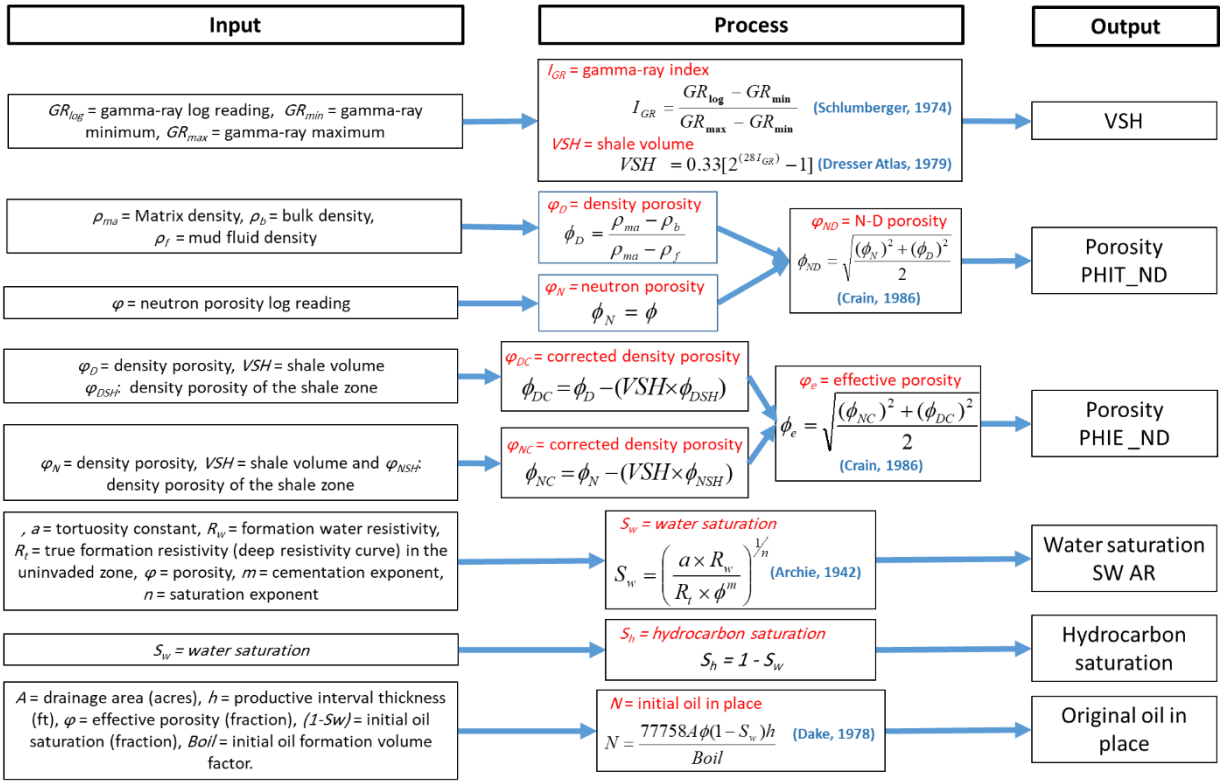

Figure 9. Workflow used for well log interpretation of AEB-III-E reservoir [45-49].

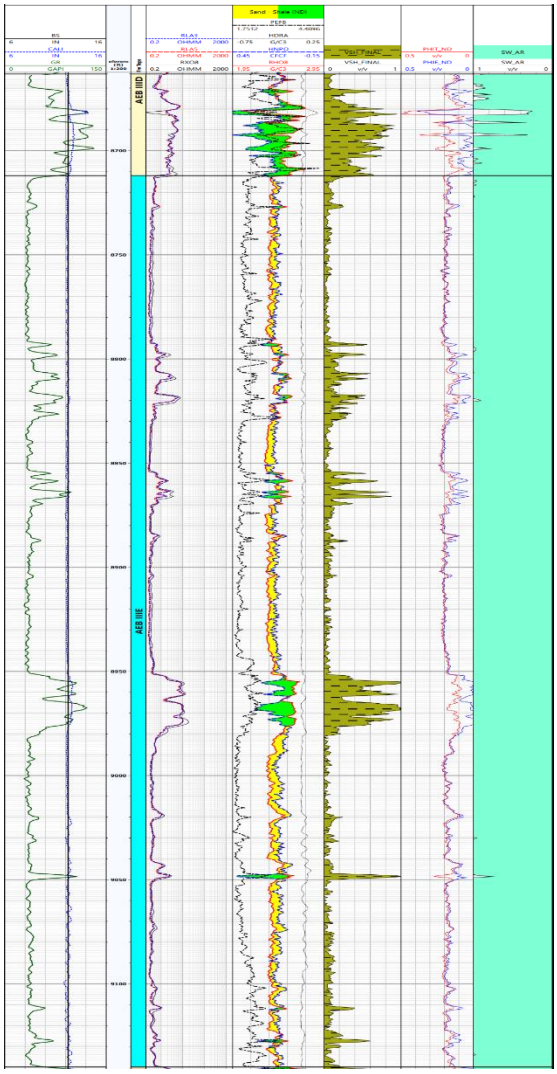

Figure 10. Logs and evaluation results of Alam El-Bueib IIIE in well J-1X.

point of view using the fault seal analysis technique which is the key to solving this mystery.

4.3. Fault seal analysis

Identifying the linkage of fault segments is a critical geometric component that connects the across-fault flow. Hydrocarbon trapping by fault sealing denotes a vital indefinite aspect in risk analysis associated with strategies of hydrocarbon exploration. In addition, fault sealing is a vital factor that controls reservoir behavior during production. Historically, the works of Smith, [51]; Schowalter, [52]; Smith, [53]; Watts, [54]; Allan, [55] and Bouvier et al., [56] were the first efforts that dealt with the fundamental concepts of hydrocarbon sealing and trapping by faults. More recently, the works of Knipe, [57-59]; Jev et al., [60]; Knott, [61]; Gibson, [62] and Berg and Avery, [63] stated the initial approaches for evaluating fault sealing. Knipe, [64] introduced the route to outline the important components for fault seal evaluation (Fig.11), in addition to the juxtaposition bases utilized for fault seal diagrams (Fig. 12a and b).

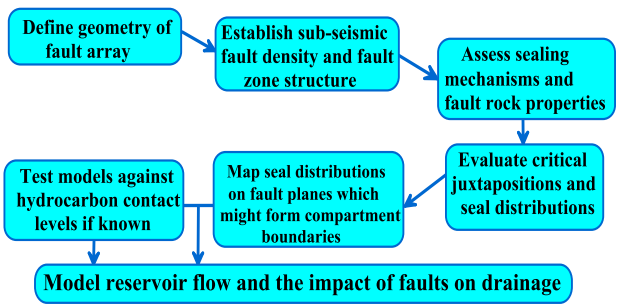

Figure 11. Important components needed for fault seal evaluation [64].

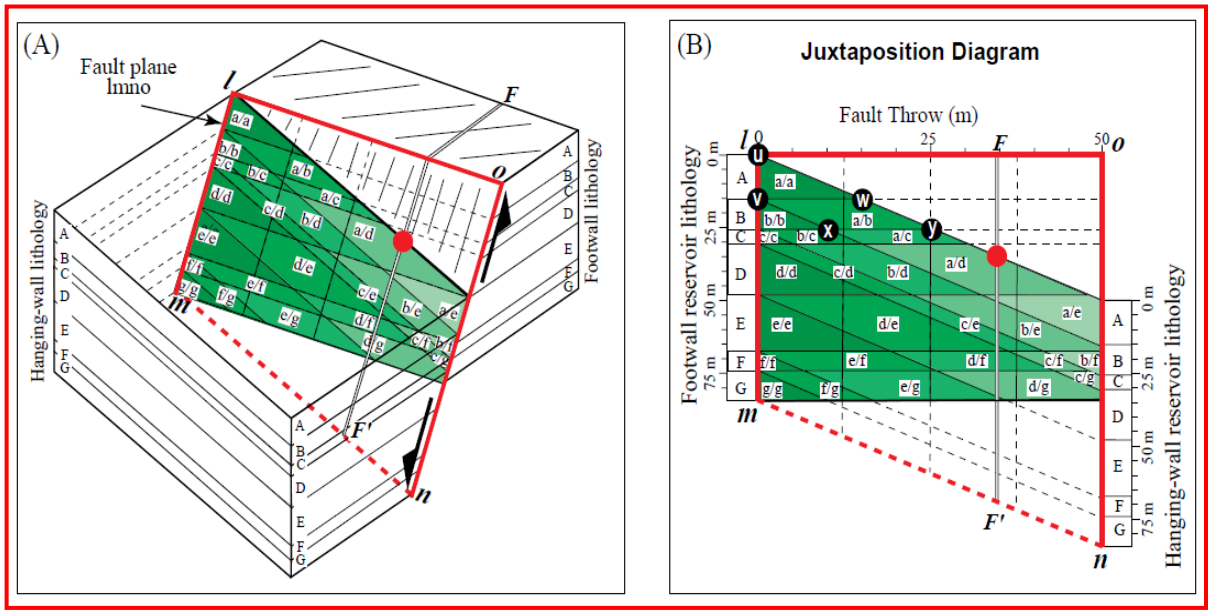

Figure 12. The bases of the juxtaposition and fault seal diagrams [64].

The fault-seal analysis technique is divided into two phases illustrated through the workflow of Figure (13). The first phase is based on the concepts of the juxtaposition of Knipe, [64; 65] which utilizes the fault-seal properties to test the leakage effect and sealing or non-sealing of the analyzed fault. The second phase uses the fault and horizon geometry in estimating the location and depth of the leakage window and finally detecting the spill pattern and estimating the depth to oil-water contact and spill point (Allan diagram, Knipe, [64]).

AEB-III-E Member is mapped in terms of time and then converted to depth using the average velocity map. The interpreted faults dissecting AEB-III-E Member are mainly trending NW-SE. The conjunction of the fault polygons with the horizon grid is used to locate and estimate the horizon cutoffs at the faults. Top AEB III-E in the upthrown and the downthrown are quoted from the depth maps, and AEB II-A, AEB II-B, AEB III-A, AEB III-C, AEB III-D, AEB III-G, AEB III-F, AEB IV, and AEB V are calculated through isopaching along the target AEB III-E fault with 250 m spacing in the "X" direction (Fig. 4a and b). This allows a 2D visualization of fault displacement and shows the point of maximum throw and the crucial sand-on-sand juxtaposition or leak points. The lithology of AEB Members is differing between sand and shale. Figure (14) illustrates the input GR log and output of Vsh of

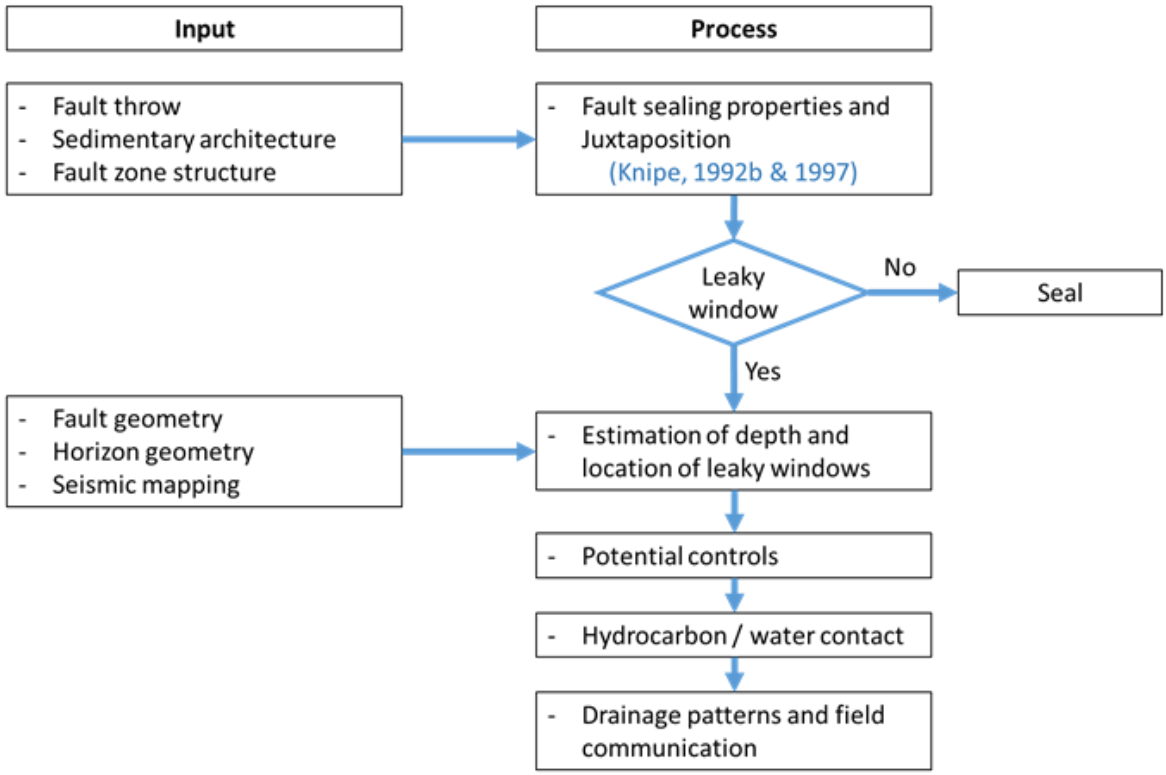

Figure 13. Workflow used for fault-seal analysis [64; 65].

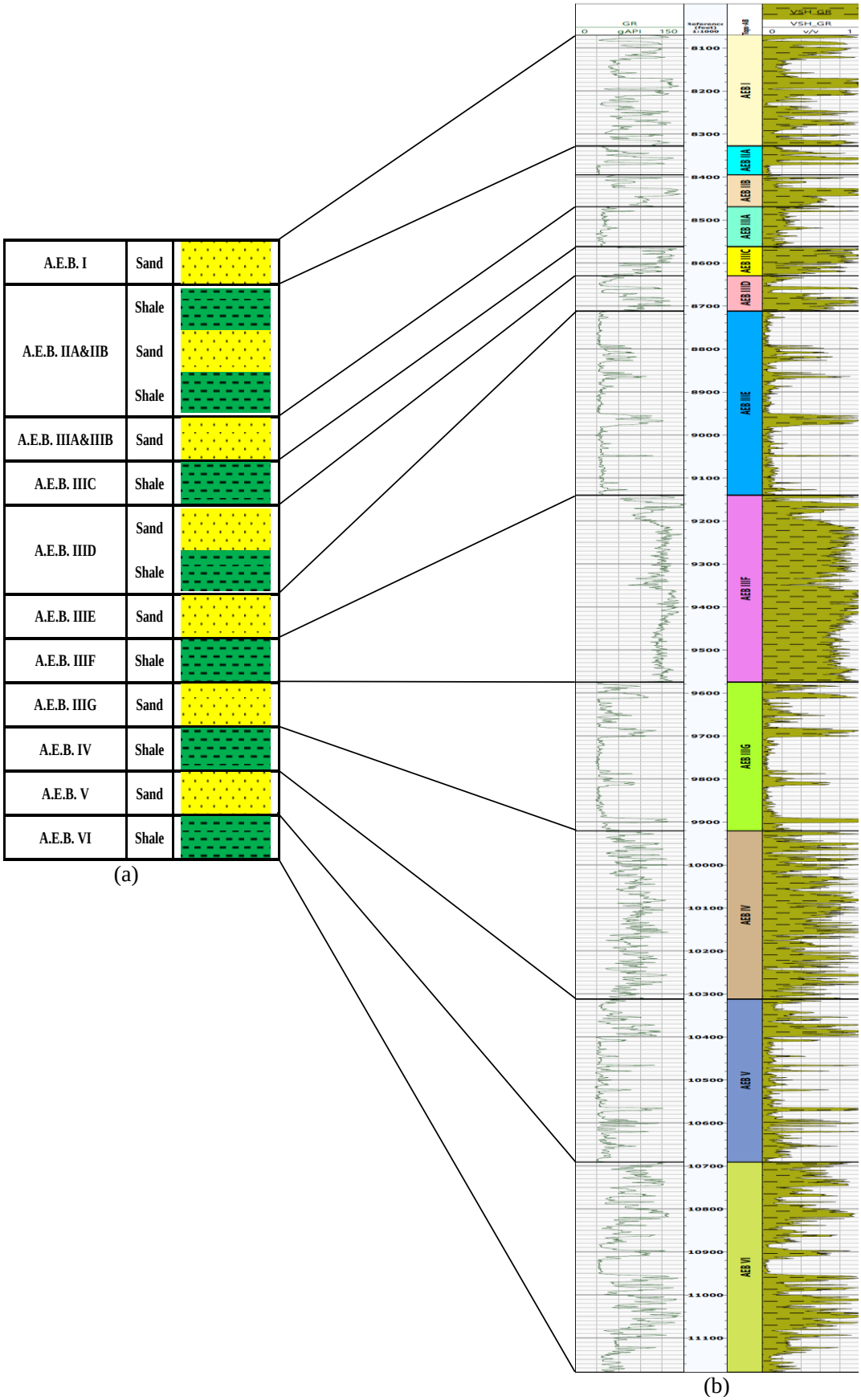

Figure 14. Simplified stratigraphic section of Alam El-Bueib Members.

the J-1X well and accordingly classifies the shale and shaly sand units of the studied AEB Formation. Allan's diagram of AEB Formation explained that the ambit between 712250X and 719500X doesn't offer any perspectivity for AEB III-B and AEB III-C later seal (Fig. 15). It is sand to the sand case across the fault plane and most probably represents the leak zone, except for the AEB III-B sand in the area extended between 715000X and 716000X that juxtapose AEB II-A shale.

For any closure, AEB III-G sand is possibly to be hydrocarbon bearing except for the area between 717500X and 718250X. For any closure, AEB IV Member is possibly to be hydrocarbon bearing except for the area between 717000X and 718500X along the

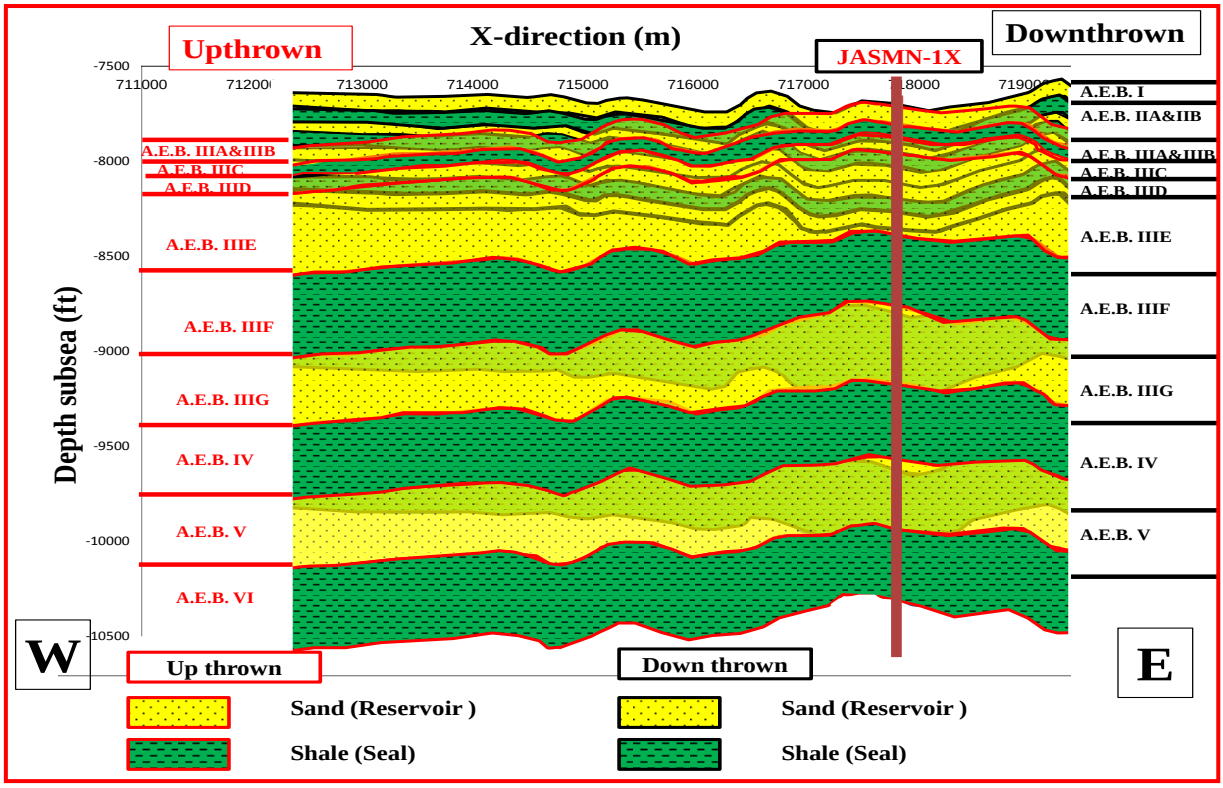

Figure 15. Allan Diagram (Bed-Fault intersections) of Alam El-Bueib fault-F1.

mentioned fault. As a result, Allan's Diagram shows that fault F1 probably represents where the location of the J-1X well is not only at the down-dip part of the member but also the point is a leaking zone. So, it represents no hydrocarbon trapping potentiality at the J-1X well. On the other hand, hydrocarbon potentiality could be found in other locations (Fig. 15).

4.4. Hydrocarbon prospects speculation

Two promising prospects are predicted for AEB-III-E Member. These prospects are analyzed and represented through the nearest seismic sections passing through them, Isochronous maps, depth maps, and 3-D structure models. The oil in place is determined for each prospect to show the potentiality for each of them. The AEB Formation is considered a reservoir in the under-investigation Aman oil field. The major two normal faults (F1-F2) bounded the horst structure in the middle. The mild horst block rotational shifting produced a shallower depth in the southern part. The area contains two possible locations which are considered a prospect. Prospect (E) shows a three-way dip closure and prospect (F) illustrates a four-way dip closure in the northern part (Fig. 16).

Through prospect (E), the seismic line 5474 was selected perpendicular to the horst structure trending N-S direction (Figs. 17 a and b). It shows that the dip closure in the F1 fault up-thrown side is a three-way type. The depth map of this prospect reflected a structure that can be classified in detail as a four-way dip closure and in regional as a three-way dip closure. This closure is bounded by the faults that trend NW-SE with a vertical closure is around 60 ft. The area of this prospect is around 2.4 sq km, the spill point is at -8100 ft and the optimum location for the drilling is at X: 713562 mE and Y: 289340 mN. The prospect (F) reflected a four-way dip closure crossed by the seismic line 2054 which is E-W oriented (Figs 18 a and b). The depth map of the prospect (F) reflected a structure that is classified in detail as a four-way dip closure with vertical closure around 40 ft. The area of the prospect (F) is around 0.75 sq. km with a spill point at -8120 ft and optimum location for the drilling at X: 715384 mE and Y: 291681 mN.

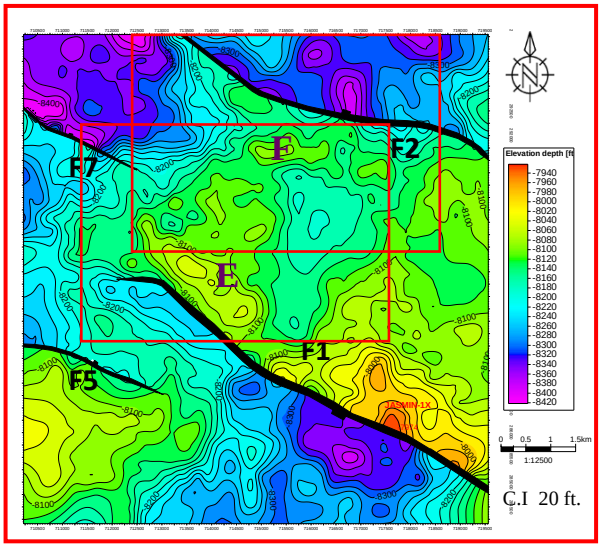

Figure 16. Depth map on top of Alam El-Bueib IIIE, showing prospects E and F.

4.5. Original oil in place of speculated new prospects.

The estimation of hydrocarbons in place or recoverable hydrocarbons is the primary goal in the selection of logs run in an exploratory or development

well. The equation of Dake [47] is utilized to provide reliable estimates of the hydrocarbons in place as shown in the workflow in Figure (9). Where AEB III-E Member is proposed as a prospect, the inferred prospects E and F are of areas 2.4 sq. km and 0.75 sq. km, and the spill points at -8100 ft and -8120 ft, respectively. As AEB III-E Member is not covered by the wireline logs, the petrophysics is not evaluated and prospects E and F of AEB III-E need more study to be evaluated in detail (Table 1).

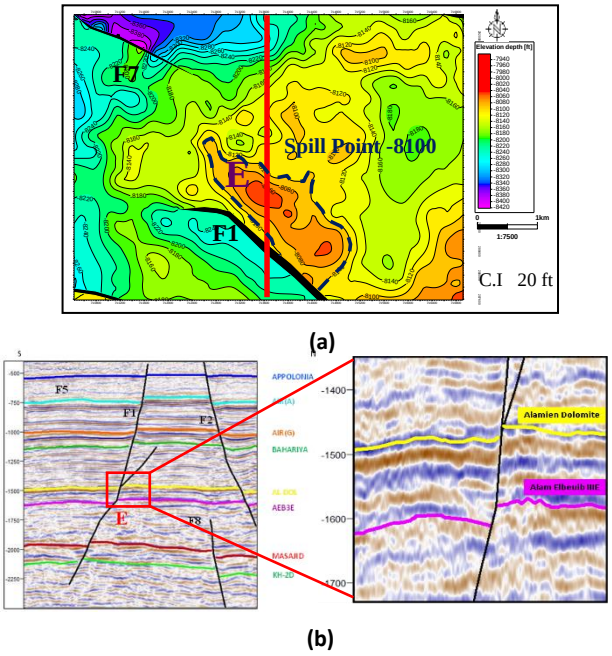

Figure 17. Depth map on top of Alam El-Bueib IIIE at the prospect E (a) and seismic line 5474 showing prospect (E) (b).

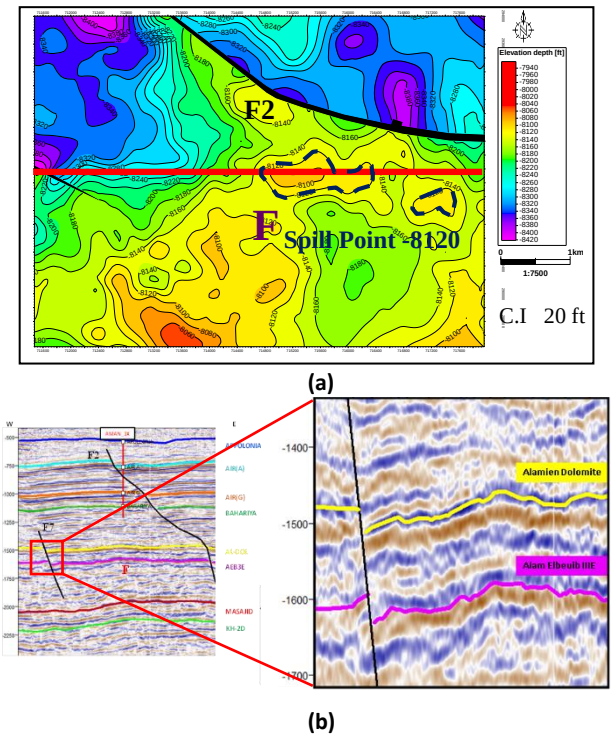

Figure 18. Depth map on top of Alam El-Bueib IIIE at the prospect F (a) and seismic line 2054 showing prospect (F) (b).

Table (1): Original oil in place (OOIP) calculation of new expected prospects and proposed new well locations.

Formation	Alam El-Bueib Formation (AEB IIIG) at JASMIN 1X Well	
Prospect	E	F
Reservoir	AEB IIIE	AEB IIIE
HC Area (km2)	2.28	0.61
Spill point depth (ft)	8100	8120
Porosity	(10-20) 14	(10-20) 14
Water saturation	49	49
Formation volume factor	1.08	1.08
Net/Gross	0.7	0.7
Prospect OOIP (Mbbl)	4.47	0.59

5. Conclusions

The inspection of structures on the top of the AEB III-E structure contour depth map and the constructed 3D structural model show general dipping to the north and south with the highest portion located in the eastern and southwestern areas of the top of AEB III-E. The top is affected by several normal faults and most of them have NW-SE trends. The structural closures and horst block faulting produces the most promising locations, in the form of mostly three-way dip and sometimes four-way dip closures, that favor the trapping of hydrocarbons in the case of AEB III-E rock units which have good reservoir characteristics.

The AEB-III-E Member consists of sandstone zones with shale and siltstone zones. The composition is suitable for hydrocarbon accumulation. AEB-III-E underlies AEB-III-D where its shale (bottom part of AEB-III-D Member) acts as a cap rock. The analysis shows that AEB-III-E Member has about 362 ft reservoir thickness with porosity of about 16 % and water saturation near 100 %. It is found that there is no hydrocarbon found in AEB III-E Member in J-1X well and this is contrary to expectations. Therefore, it was necessary to re-study from another point of view. From the authors' point of view, using the fault seal analysis technique may be the key to solving this mystery in this study.

The Allan Diagram is conducted to emphasize the fault-seal analysis and petrophysical characteristics of reservoirs of the study area to develop its hydrocarbon trapping potentiality. Allan's Diagram shows that the fault F1 probably represents where the location of the J-1X well is not only at the down-dip part of the member but also at the point of its leak zone. So, it represents no hydrocarbon potentiality at the J-1X well. On the other hand, hydrocarbon potentiality could be found in other locations. The

structure contour map of AEB-III-E Member illustrated two promising prospects in the northern part. The prospect (E) shows a three-way dip closure with height of 60 ft and area of about 2.4 sq km. The prospect (F) reflected a four-way dip closure with height of 40 ft and area of around 0.75 sq. km.

Funding sources

This research received no external funding.

Conflicts of interest

On behalf of all authors, the corresponding author states that there is no conflict of interest.

Acknowledgments

The authors are wishing to thank the EGPC and Agiba Petroleum Company for permitting the use of data in this study. We appreciate Schlumberger for helping and providing us with the license of the software. We appreciate the critical discussion of the practice by Geophysicist Dr. Nashat S. Gawish and Geophysicist / Ahmed Bakry for their valuable comments.

References

[1] J. E. Cheng, Petroleum System of Shoushan Basin, Western Desert, Egypt. Geological Behavior, Acta Scientifica Malaysia (ASM), 4 (1), (2020), pp. 01-08.

[2] M. F. Abu-Hashish, M. Abuelhassan, A. Said, Analysis of the Petroleum System Elements of the Amana Oil Field, East Abu Gharadig Basin, Western Desert, Egypt. Journal of Petroleum and Mining Engineering, 24 (1), (2022), pp. 28-41. https://doi. org/10.21608/jpme.2022.125833.1117

[3] Globe Task Team et al., The Global Land One-kilometer Base Elevation (GLOBE) Digital Elevation Model, Version 1.0, D.A. Hastings, P.K. Dunbar, G.M. Elphingstone, M. Bootz, H. Murakami, H. Maruyama, H. Masaharu, P. Holland, J. Payne, N.A. Bryant, T.L. Logan, J.-P. Muller, G. Schreier, and J.S. MacDonald, eds.: National Oceanic and Atmospheric Administration, National Geophysical Data Center, 325 Broadway, Boulder, Colorado 80303, U.S.A. Digital data base on the World Wide Web (URL: http://www.ngdc.noaa.gov/mgg/topo/globe.html) and CDROMs (1999).

[4] W. H. F. Smith, D.T. Sandwell, Global sea floor topography from satellite altimetry and ship depth soundings: Science Magazine, v. 277, (1997), pp. 1956-1962.

[5] W. Bosworth, A.S. El-Hawat, D.E. Helgeson, K. Burke, Cyrenaican “shock absorber” and associated inversion strain shadow in the collision zone of northeast Africa: Geology, v. 36, (2008)pp. 695-698.

[6] (EGPC) Egyptian General Petroleum Corporation, Exploration and production review (part 1), Western Desert, oil and gas fields, (a comprehensive overview). in: 11th EGPC Petrol. Explor and Prod. Conf. Cairop. (1992) 431p.

[7] M. Darahem, G. Paradisi, Aman field. A case history of field development under complex reservoir geology conditions. in: 11th EGPC Explor. and Prod. Conf. 2, (1992) pp. 324-336.

[8] A. R. Moustafa, Mesozoic-Cenozoic basin evolution in the northern Western Desert of Egypt, In: Solem, M., El-Arnouti, A., and Saleh, A. (eds), 3fd Symposium on the sedimentary basins of Libya (TheGeology of East Libya), v. 3, (2008) pp. 29-46.

[9] Schlumberger, Well evaluation conference, Egypt. Schlumberger Technical Editing Services, Chester, (1995) pp. 58-66.

[10] A. R. Moustafa, A. N. El-Barkooky, A. Mahmoud, A. M. Badran, M. Nour El-din, H. Fathy, Mature basin hydrocarbon plays in an inverted Jurassic-Cretaceous rift basin in the northern Western Desert of Egypt, Am Assoc. Petrol. Geol. Int. meeting (Cairo, Oct. 2002), Abstract (2002).

[11] M. M. El Nady, Evaluation of the nature, origin and potentiality of the subsurface Middle Jurassic and Lower Cretaceous source rocks in Melleiha G-1x well, North Western Desert, Egypt. Egyptian Journal of Petroleum, 24(3), (2015) pp. 317-323. Doi:10.1016/j.ejpe.20 15.07.012.

[12] M. G. Temraz, D. A. Mousa, M. A. Lotfy, Evaluation of the shale beds within Alam El Bueib Formation as an unconventional reservoir, Western Desert, Egypt. J Petrol Explor Prod Technol, 8 (2018) pp. 43-49. https://doi.org/10.1007/s13202-017-0353-z.

[13] M. Fagelnour, I. Gamil, M. El Toukhy, A. Gharieb, H. Saad, Source rock potentiality, basin modeling, and oil to source correlation in northern Shushan Basin, Western Desert, Egypt. Offshore Mediterranean Conference and Exhibition, 27-29 March, Ravenna, Italy (2019).

[14] W. A. Makled, A. Abd El Moneim, T. F. Mostafa, M. Z. El Sawy, D. A. Mousa, M. O. Ragab, Petroleum play of the Lower Cretaceous Alam El Bueib Formation in the El Noor-1X well in the north Western Desert (Egypt): A sequence stratigraphic framework. Marine and Petroleum Geology 116, 104287 (2020). Doi.org/10.1016/j.marpetgeo.2020.1042 87.

[15] S. M. T. Qadri, M. A. Islam, M. R. Shalaby, A. K. Eahsanul-Haque, Seismic interpretation and structural modeling of Kupe field, Taranaki Basin, New Zealand. Arabian Journal of Geosciences, 10, (2017) 295 p.

[16] M. Abdel-Fattah, F. Metwalli, E. Mesilhi, Static reservoir modeling of the Bahariya reservoirs for the oil fields development in South Umbarka area, Western Desert. Egypt. Journal of African Earth Sciences, 138, (2018) pp. 1-13.

[17] M. K. Barakat, N. H. El-Gendy, M. A. El-Bastawesy, Structural modeling of the Alam El-Bueib Formation in the Jade oil field, Western Desert, Egypt. Journal of African Earth Sciences, 156, (2019) pp. 168-177.

[18] A. O. Adelu, A. A. Aderemi, A. O. Akanji, O. A. Sanuade, S. I. Kaka, O. Afolabi, Application of 3D static modeling for optimal reservoir characterization. Journal of African Earth Sciences, 152, (2019) pp.184-196.

[19] B. Issawi, M. H. Francis, E. A. A. Youssef, R. A. Osman, The Phanerozoic geology of Egypt, a geodynamic approach, 2nd ed. Ministry of Petroleum, The Egyptian Mineral Resources Authority, Special Publication, Cairo, (2009) pp. 589.

[20] R. Said, The geology of Egypt. Rotterdam, Netherlands, A.A. Balkema Publishers, (1990) 734 p.

[21] G. Hantar, North Western Desert. In: The geology of Egypt. (Ed. R. Said, 1990). Balkema Publishers, (1990) pp. 293-319.

[22] B. Issawi, M. El Hinnawi, M. Francis, A. Mazhar, The Phanerozoic geology of Egypt: a geodynamic approach. Egyptian Geological Survey, Paper 76 (1999) p. 462.

[23] A. R. Moustafa, A. Saoudi, A. Moubasher, I. M. Ibrahim, H. Molokhia, B. Schwartz, Structural setting and tectonic evolution of the Bahariya Depression, Western Desert, Egypt. Gulf PetroLink, Bahrain, GeoArabia, Vol. 8, No. 1, (2003) pp. 91-124.

[24] A. El Awdan, F. Youssef, A. R. Moustafa, Effect of Mesozoic and Tertiary deformations on exploration in the northern Western Desert, Assoc. Petrol. Geol. Int. meeting (Cairo, Oct. (2002).

[25] M. M. Gadallah, A. Samir, M. A. Nabih, Integrated reservoir characterization studies of Bahariya Formation in the Meleiha-NE Oil Field, North Western Desert, Egypt, 10.4197 / Ear. 21-1.5, JKAU: Earth Sci., Vol. 21, No. 1, (2009) pp. 111-136.

[26] J. C. Dolson, M. Atta, D. Blanchard, A. Sehim, J. Villinski, T. Loutit, K. Romine, Egypt's future petroleum resources: A revised look into the 21st century,in L. Marlow, C. Kendall and L. Yose, eds., Petroleum systems of the Tethyan region: AAPG Memoir 106, (2014) pp.143-178. https://doi.org/10.1306/M1061343

[27] M. Abdel-Fattah, M. Gameel, S. Awad, A. Ismaila, Seismic interpretation of the Aptian Alamein Dolomite in the Razzak oil field, Western Desert, Egypt. Arab J Geosci 8, 4669-4684(2015). https://doi.org/10.1007/s12517-014-1595-4

[28] W. Bosworth, M. A. Abrams, M. Drummond, M. Thompson, Jurassic rift initiation source rock in the Western Desert, Egypt– relevance to exploration in other continental rift systems. Proceeding 34th Annu. GCSSEPM Found. Bob F. Perkins Res.Conf. Pet. Syst. "rift" basins, (2015) pp. 615-650. https://doi.org/10.5724/gcs.15.34.0615

[29] S. S. Azzam, H. H. El Kady, T. M. Rabea, The impact of seismic interpretation on the hydrocarbon trapping at Falak field, Meleiha, Western Desert, Egypt,Egyptian Journal of Petroleum, V. 27, I. 4, (2018) pp. 785-793. https://doi.org/10.1016/j.ejpe.2017.11.0 06.

[30] M. A. El Sherief, M. A. Elbastawesy, A. L. Abdeldayem, S. A. Mohamed, Jurassic-Lower Cretaceous petroleum system of Faghur Basin, North Western Desert, Egypt. Arab J Geosci 15, 1465, (2022). https://doi.org/10.1007/s12517-022-10661-x

[31] M. C. Cacas, J. M. Daniel, J. Letouzey, Nested geological modelling of naturally fractured reservoirs. Petroleum Geoscience, 7, (2001) pp. S43-S52.

[32] P. Meldahl, R. Heggland, B. Bril, , P. de Groot, Identifying faults and gas chimneys using multiattributes and neural networks. The Leading Edge, 20, (2001) pp. 474–482.

[33] G. Manatschal, New models for evolution of magma-poor rifted margins based on a review of data and concepts from West Iberia and the Alps. International Journal of Earth Sciences, 93, (2004) pp. 432-466.

[34] D. Franke, Rifting, lithosphere breakup and volcanism: Comparison of magma-poor and volcanic rifted margins. Marine and Petroleum Geology, 43, (2013) pp. 63-87.

[35] A. Rotevatn, C. A. L. Jackson, 3D structure and evolution of folds during normal fault dip linkage. Journal of the Geological Society, 171, (2014) pp. 821-829.

[36] M. Choudhuri, M. Nemčok, C. Stuart, et al., 85° E Ridge, India – constraints on its development and architecture. Journal of the Geological Society of India, 84, (2014) pp. 513-530.

[37] A. A. Misra, Sheared Nature of the Indian Western Continental Margin around Mumbai, India: Onshore and Offshore Geoscientific Studies. PhD Thesis, Indian Institute of Technology Bombay, India (2015).

[38] H. Van Gent, S. Back, J. L. Urai, P. Kukla, Small-scale faulting in the Upper Cretaceous of the Groningen block (The Netherlands): 3D seismic interpretation, fault plane analysis and regional paleostress. Journal of Structural Geology, 32, (2010) pp. 537-553.

[39] C. Baudon, J. Cartwright, 3D seismic characterization of an array of blind normal faults in the Levant Basin, Eastern Mediterranean. Journal of Structural Geology, 30, (2008) pp. 746-760.

[40] S. Pochat, S. Castelltort, G. Choblet, J. Van Den Driessche, High-resolution record of tectonic and sedimentary processes in growth strata. Marine and Petroleum Geology, 26, (2009) pp. 1350-1364.

[41] G. D. Kidd, Fundamentals of 3-D seismic volume visualization, the leading edge, vol. 18, (1999) pp. 702-712.

[42] Schlumberger, Log interpretation charts. Schlumberger Ltd., (1989) pp. 74-105.

[43] Schlumberger, Log Interpretation Charts, Schlumberger, Sugar Land (2009).

[44] R. M. Bateman, Open hole log analysis and formation evaluation. Second Edition, Society of Petroleum Engineers (SPE), ISBN 978-1-61399-156-5, ISBN 978-1-61399-269-2 (Digital), 653(2012).

[45] G. E. Archie, The electrical resistivity log as an aid in determining some reservoir characteristics. Transactions of the AIME, 146(01) (1942) pp.54-62. Doi:10.2118/942054-g.

[46] Schlumberger, Log interpretation manual/applications. Vol. 2: Houston, Schlumberger Well Services, Inc (1974).

[47] L. P. Dake, Fundamentals of reservoir engineering, Developments in Petroleum Science, 0-444-41830-X, Elsevier science B.V. All rights reserved 499(1978).

[48] Dresser Atlas, (1979) Log interpretation charts: Houston. Texas, Dresser Industries Inc, 107.

[49] E. R. Crain, The log analysis handbook. Penn-Well Publishing Company, Tulsa, Oklahoma, USA, (1986).

[50] F. I. Metwalli, J. D. Pigott, F. S. Ramadan, A. A. El-Khadragy, W. A. Afify, Alam El Bueib reservoir characterization, Tut oil field, North Western Desert, Egypt. Environ Earth Sci 77, 143(2018). https://doi.org/10.1007/s12665-018-7290-0

[51] D. A. Smith, (1966) Theoretical consideration of sealing and non-sealing faults, Am. Assoc. Pet. Geol. Bull., 50, pp. 363-374.

[52] T. T. Schowalter, Mechanisms of secondary hydrocarbon migration and entrapment, Am. Assoc. Pet. Geol. Bull., 63, (1979) pp. 723-760.

[53] D. A. Smith, Sealing and non-sealing faults in Louisiana Gulf Coast salt basin, Am. Assoc. Pet Geol. Bull., 64, (1980) pp.145-172.

[54] N. L. Watts, Theoretical aspects of cap-rock and fault seals for single and two-phase hydrocarbon columns. Mar. Petroleum geology, 4, (1987) pp. 274-307.

[55] U. S. Allan, Model for hydrocarbon migration and entrapment within faulted structures, Am. Assoc. Pet. Geol. Bull., 73, (1989) pp. 803-811.

[56] J. D. Bouvier, K. Sijpesteijn, D. F. Kluesner, C. C. Onyejekwe, R. C. Van Der Pal, Three-dimensional seismic interpretation and fault sealing investigations, Nun River field, Nigeria, Am. APPG. Bull., 73, (1989) pp. 1397-1414.

[57] R. J. Knipe, Faulting processes and fault seal. Larsen, R. M., Brekke, H., Larsen, B. T. and Talleraas E. (Editors), Structural and Tectonic Modelling and its Application to Petroleum Geology, NPF Special Publication 1, Stavanger, (1992a) pp. 325-342.

[58] R. J. Knipe, The influence of fault zone processes and diagenesis on fluid flow, Horbury, A. D., and Robinson, A. G. (Editors), Diagenesis and Basin Development, Am. Assoc. Pet. Geol. Studies in Geology, 36. American Association of Petroleum Geologists, Tulsa, OK, (1993a) pp. 135-154.

[59] R. J. Knipe, Micromechanisms of deformation and fluid behavior during faulting, The Mechanical Involvement of Fluids in Faulting. USGS, Open-File Report 94-228, (1993b) pp. 301-310.

[60] B. I. Jev, C. H. Kaars-Sijpesteijn, M. P. A. M. Peters, N. L. Watts, J. T. Wilkie, Akaso field, Nigeria, use of integrated 3-D seismic, fault slicing, clay smearing, and RFT pressure data on fault trapping and dynamic leakage, Am. Assoc. Pet. Geol. Bull.,77, (1993) pp. 1389-1404.

[61] S. D. Knott, Fault seal analysis in the North Sea. Am. Assoc. Pet. Geol. Bull., 77, (1993) pp. 778-792.

[62] R. G. Gibson, Fault-zone seals in siliclastic strata of the Columbus Basin, Offshore Trinidad Am. Assoc. Pet. Geol. Bull., 78, (1994) pp. 1372-1385.

[63] R. B. Berg, A. H. Avery, Sealing properties of Tertiary growth faults, Texas Gulf coast, Am. Assoc. Pet. Geol. Bull., 79 (1995)pp. 375-393.

[64] R. J., Knipe, Juxtaposition and seal diagrams to help analyze fault seals in hydrocarbon reservoirs. Am. Assoc. Pet. Geol. Bull., 81 (1997), pp. 187-195.

[65] R. J. Knipe, Faulting processes, seal evolution and reservoir discontinuities, an integrated analysis of the ULA Field, Central Graben, North Sea, Abstracts of the Petroleum Group Meeting on Collaborative Research Program in Petroleum Geoscience between UK Higher Education Institutes and the Petroleum Industry, Geological Society, London, (1992b).